JTTEE5 23:182–189
DOI: 10.1007/s11666-013-9971-2
1059-9630/$19.00 © ASM International

Improved Thermal Cycling Durability of Thermal Barrier Coatings Manufactured by PS-PVD

S. Rezanka, G. Mauer, and R. Vaßen

(Submitted April 29, 2013; in revised form June 26, 2013)

The plasma spray-physical vapor deposition (PS-PVD) process is a promising method to manufacture thermal barrier coatings (TBCs). It fills the gap between traditional thermal spray processes and electron beam physical vapor deposition (EB-PVD). The durability of PS-PVD manufactured columnar TBCs is strongly influenced by the compatibility of the metallic bondcoat (BC) and the ceramic TBC. Earlier investigations have shown that a smooth BC surface is beneficial for the durability during thermal cycling. Further improvements of the bonding between BC and TBC could be achieved by optimizing the formation of the thermally grown oxide (TGO) layer. In the present study, the parameters of pre-heating and deposition of the first coating layer were investigated in order to adjust the growth of the TGO. Finally, the durability of the PS-PVD coatings was improved while the main advantage of PS-PVD, i.e., much higher deposition rate in comparison to EB-PVD, could be maintained. For such coatings, improved thermal cycling lifetimes more than two times higher than conventionally sprayed TBCs, were measured in burner rigs at ~1250 °C/1050 °C surface/substrate exposure temperatures.

Keywords low pressure plasma spray (LPPS), PS-PVD, pre-heating of substrate, thermal cycling, thermal cyclic properties, vacuum plasma spray

1. Introduction

The plasma spray-physical vapor deposition (PS-PVD) process, which was primarily named as low pressure plasma spraying-thin film process (LPPS-TF), was developed in several steps. The original low pressure plasma spray process (LPPS), which is also known as vacuum plasma spray process (VPS), operates at 5-20 kPa. The very low pressure plasma spray process (VLPPS) was established by further decreasing the working pressure to 50-200 Pa. Thereby uniform and thin coatings could be deposited with large area of coverage. PS-PVD was established by the addition of enhanced electrical input power to the VLPPS process (Ref 1-3).

Increased power input and heat transfer to the powder causes not only melting but also vaporizing of the material. Furthermore a situation between liquid and vapor deposition exists, in which nano-sized clusters are deposited (Ref 4). This deposition of clusters enables the formation of columnar microstructures which are unique for thermal spray processes and similar to the structures obtained by EB-PVD (Ref 2-4). One important application of this process is the manufacturing of thermal barrier coatings (TBCs). Currently, these ceramic protection layers on gas turbine components are deposited either by atmospheric plasma spraying (APS) or by EB-PVD. PS-PVD combines the main advantages of both processes. The columnar microstructures provide a high strain tolerance. However, EB-PVD is expensive. In contrast, the manufacturing costs of PS-PVD are comparatively low (Ref 4). Initial experiments, nonetheless showed lower lifetimes in burner rig tests compared to TBCs manufactured by APS (Ref 4). In this work, the lifetime of TBCs made by PS-PVD was increased by an adjusted processing, in particular the introduction of coating steps with low deposition rates and enhanced pre-oxidation of the bondcoat (BC) surface.

2. Experimental Procedures

The facility used in the experiments is a Sulzer Metco Multicoat system (Sulzer Metco, Wohlen, Switzerland), which was obtained by reconstruction of a conventional LPPS system. By the addition of a second vacuum pumping unit and a large vacuum blower, the pumping capacity at the PS-PVD working pressures of 50-200 Pa was enhanced. To achieve an electrical input power of up to 180 kW, which is needed for PS-PVD, three new power sources and a new cooling system with up to 90 kW cooling capacity were installed. Also a new torch transfer system, which allows spray distances up to 1500 mm and a

This article is an invited paper selected from presentations at the 2013 International Thermal Spray Conference, held May 13-15, 2013, in Busan, South Korea, and has been expanded from the original presentation.

S. Rezanka, G. Mauer, and **R. Vaßen**, Forschungszentrum Jülich GmbH, Institut für Energie- und Klimaforschung: Werkstoffsynthese und Herstellungsverfahren (IEK-1), 52425 Jülich, Germany. Contact e-mail: s.rezanka@fz-juelich.de.

new control system were established. For PS-PVD operation a modified single cathode O3CP gun is used, but the system can also be operated with a F4-VB torch and a three-cathode TriplexPro torch (all by Sulzer Metco, Wohlen, Switzerland).

The feedstock material was an agglomerated 7 wt.% yttria partially stabilized zirconia powder (7YSZ) produced by Sulzer Metco designated as M6700. The grain size distribution obtained by laser diffraction measurements were: $d_{10} = 2$ µm, $d_{50} = 8$ µm, and $d_{90} = 18$ µm.

Disks made of Inconel IN738, with a diameter of 30 mm and a thickness of 3 mm, were used as substrates. The topside edge of the specimens was rounded and a hole for a thermocouple and a groove for clamping were machined. A schematic drawing of a thermal cycling specimen is shown in Fig. 1.

Before the application of the TBC, the substrates were coated with a 200 µm thick BC using LPPS. The BC materials were NiCoCrAlY (Ni 192-8, Praxair GmbH) and CoNiCrAlY (Amdry 386, Sulzer Metco).

The surfaces of the BCs were ground to a surface roughness of around 0.06 µm (R_a). The remaining BC thickness was about 150 µm. The improvement of lifetime by a decreased roughness, which was reported for EB-PVD coatings, is observed to apply also for PS-PVD coatings (Ref 4). For microscopic studies, plates of stainless steel were prepared and coated similar to the Inconel specimens.

Before TBC deposition, the specimens were heated up in the vacuum chamber by the plasma jet. During the pre-heating and coating, a flow of 4 standard liters per minute (slpm) oxygen was led into the chamber. Such procedure is also reported to increase the durability of EB-PVD coatings. It is assumed that during pre-oxidation a thin α-alumina layer is formed on the BC (Ref 4). It was found that a specimen surface temperature between 1050 and 1100 °C during pre-heating and coating is beneficial for a longer lifetime of the coating system.

During the coating process, an additional oxygen flow was used to prevent a loss of oxygen in the deposited ceramic driven by the reducing conditions in the low pressure plasma plume. To further increase the durability of PS-PVD coatings, the deposition rate was reduced at the beginning of the deposition. The deposition rate was controlled by the feed rate.

PS-PVD-TBCs are usually manufactured with a deposition rate of 14.5 µm/min. Several coating procedures were investigated during this work, featuring varied deposition rates and durations of coating steps. All investigated procedures are listed in Table 1. In the first series of coatings (procedure A in Table 1) the deposition rate at the beginning of the coating process was reduced to 2.1 µm/min. The coating process was continued to a reasonable coating thickness with the usual deposition rate after an intermediate step with a deposition rate of 7.3 µm/min. One sample was already manufactured using this procedure and successfully tested in Ref 4. To increase the desired effect, the deposition rates at the beginning of the coating process and the duration of the working steps were varied in procedure B-E.

The higher deposition rate of PS-PVD compared to EB-PVD was principally maintained because only the deposition rate at the beginning of the coating process was changed.

Additionally to the reduced initial deposition rates, the pre-heating time of the specimens with the plasma plume under oxygen inlet (4 slpm) was changed to 10 min in all procedures, to increase the effect of the BC surface pre-oxidation.

Table 1 Procedures used in sample preparation using PS-PVD process with the Sulzer Metco O3CP gun, all procedures include an enhanced pre-oxidation

Procedure	Deposition rate, µm/min	Duration of step
A	2.1	1 min+
	7.3	2 min+
	14.5	Continued
B	1.1	1 min+
	4.9	2 min+
	14.5	Continued
C	2.1	5 min+
	7.3	5 min+
	14.5	Continued
D	2.1	20 min+
	7.3	2 min+
	14.5	Continued
E	14.5	Whole process

Table 2 Double-layer thermal barrier coatings

PS-PVD-layer	APS-layer
250 µm	400 µm
250 µm	400 µm (with segmentation cracks)
350 µm	50 µm

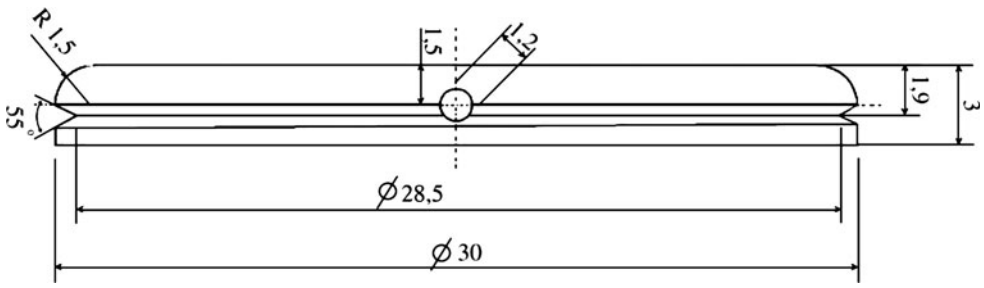

Fig. 1 Schematic drawing of thermal cycling specimen

The plasma characteristics of the used parameter, 35 slpm Ar and 60 slpm He, are described in (Ref 5). All coatings of this work were processed with a torch current of 2600 A, but during the pre-oxidation and the steps with reduced deposition rate a current of 2400 A was set.

PS-PVD-TBCs usually fail at the interface between the BC and TBC (Ref 6). One approach to overcome this weakness was to use double-layer systems with a bottom TBC layer made by APS and a PS-PVD TBC top layer. In contrast to PS-PVD the adhesion mechanism of the APS-coatings is mechanical clamping. Because of this the surface of the BC was not ground in the case of the double-layer systems. For the APS-coatings, a A3000 facility, a Triplex II gun and YSZ 204 NS powder (all by Sulzer Metco, Wohlen, Switzerland) were used. The plasma parameters were 50 slpm Ar and 4 slpm He and a torch current of 470 A. Three different double-layer systems were investigated which are listed in Table 2. First, a 250 μm thick PS-PVD TBC layer was applied on a 400 μm thick APS TBC layer. In a second trial, an APS TBC layer with segmentation cracks was chosen for a higher strain tolerance. In this work the surface roughness of the APS-coatings was not modified. This could be an improvement in the future.

Finally, a system with a thin APS TBC layer (50 μm) was chosen, because a thin APS TBC layer might be sufficient to improve the adherence of the ceramic coatings to the BC.

Besides the manufacturing of thermal cycling specimens, an experiment to coat a geometry similar to a turbine vane was performed. A small turbine vane (55 × 46 × 20 mm) mock-up close to real geometries was machined from stainless steel. This part was rotated (60 rotations per minute) during deposition and coated with a feed rate of 16 g/min and a current of 2600 A.

Thermal cycling tests were performed in a burner rig. The temperature of the specimen was set to 1250 °C on the surface and to 1050 °C on the backside. The latest specimens were tested at 1400 °C/1050 °C because of the high durability of the specimens and long test durations. A detailed test description can be found elsewhere (Ref 7).

3. Results and Discussion

3.1 As-Sprayed Microstructures

In Fig. 2 an overview of the microstructure of a specimen manufactured with procedure A is shown featuring the typical structure of PS-PVD coatings with its feather-like columns (see Ref 3 and 4 for comparison).

Figure 3 shows a detail of the bottom area of the TBC coating and of the interface between the BC and TBC.

In the BC the blocky structures of β-phase are observed. On the top of the BC a TGO layer was formed during the pre-oxidation. In this oxide layer white precipitations are found, that show high yttria, hafnium, and aluminum contents, confirmed by EDS measurements. Therefore it is suggested that these precipitations are yttrium aluminates.

Hospach et al. described the growth of a columnar structured layer (Ref 3). At the interface, initial columns with widths of few μm are deposited which make the interface look very dense. During the continued deposition, some columns grow faster than the others and the slower growing crystals stop when they come close to their neighbor. Thereby the gaps between the columns which lead to the increased tolerance to strain are formed. Looking at the bottom areas of the TBC coatings deposited with a low feed rate, it seems that this dense layer is more pronounced. Not only the interface layer but also the inner areas and the ''feathers'' of the columns near the interface look denser. Figure 4 presents a scanning electron micrograph of a coating deposited with procedure C.

The interface layer of this coating seems even denser and its thickness seems to be higher than that of procedure

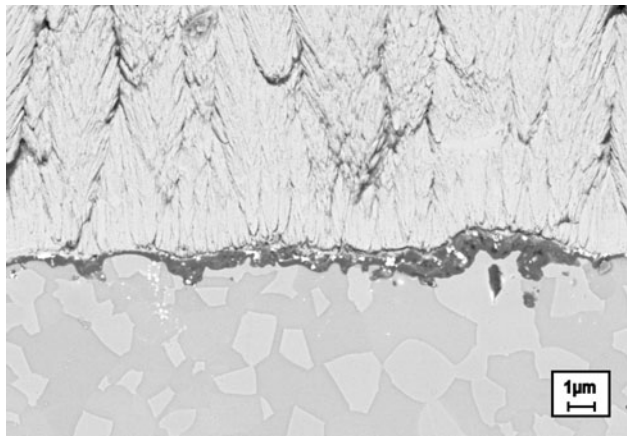

Fig. 3 Scanning electron micrograph (back-scattered electron image) of coating deposited with procedure A (interface)

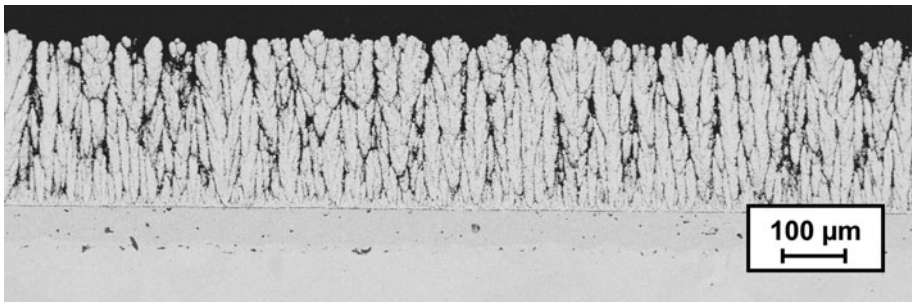

Fig. 2 Scanning electron micrograph (back-scattered electron image) of a coating deposited with procedure A (overview)

A. Thus, the thickness of the denser layer of the coatings produced with low deposition steps seem to be influenced by the design of these steps. A lower deposition rate makes the zone appear denser and the thickness of the zone seems to be increased by a longer period of low deposition processing.

As reported in Ref 3 and 6 a denser layer is observed in every PS-PVD microstructure and its thickness varies even for same processing; the reasons are still not completely clarified. Because of this, a quantitative correlation between the feed rates and durations of the low deposition steps and the thickness of the denser layers could not be established yet.

A scanning electron micrograph of a double-layer coating with the thinnest chosen APS-layer is shown in Fig. 5. The columns of PS-PVD coatings start to grow on the highest points of a rough surface (Ref 6). In the double-layer structure, the columns start from the highest splats on the top of the APS-layer. As a result, the columns have a larger distance between each other and grow wider compared to PS-PVD coatings on smooth surfaces.

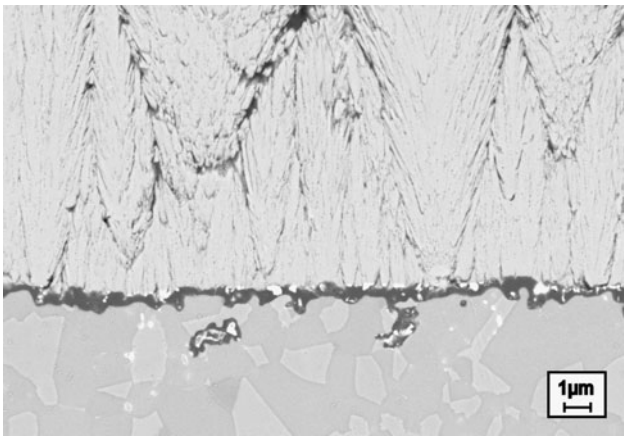

Fig. 4 Scanning electron micrograph (back-scattered electron image) of coating deposited with procedure C (interface)

3.2 Thermal Cycling Lifetimes

In Fig. 6, the results of the burner rig tests are plotted. The duration of the heating phase in thermal cycling was used to convert the number of cycles into time at high temperature. During testing the temperatures at the surface of the specimens and at their backside were measured by pyrometer and thermocouple in the substrate respectively. Using a simple layer model and assuming a thermal conductivity of 1.2 W/m·K for the PS-PVD TBC layer and 1.0 W m·K for the APS TBC layer (Ref 4), the temperature at the interface between the BC and TBC was calculated based on the measured temperatures. In Fig. 6, the thermal cycling time is plotted against the inverse BC temperature. This plot simplifies the comparison of different test conditions. In Ref 5, a linear correlation between the inverse BC temperature and the lifetime is established. The lifetimes of the double-layer coatings are between 100 and 200 h in tests at 1250 °C/1050 °C (surface/substrate temperature) and thereby in the range of usual APS-coatings. However, the lifetimes of the PS-PVD coatings with pre-oxidation and low deposition steps are between 10 h (procedure E without low deposition step) and 400 h (procedure A) in tests at 1250 °C/1050 °C and 1400 °C/1050 °C (the highest lifetimes are observed at 1250 °C/1050 °C).

Thus, the columnar microstructure and thereby the improved strain tolerance of the PS-PVD coatings leads to a large improvement in durability (almost a factor of two). A further improvement of durability compared to earlier PS-PVD-coatings (Ref 3, 4) seems to be obtained by the introduction of the steps with low deposition rates and of the pre-oxidation. However, these effects are still not understood in detail. It is assumed that the precipitation of yttrium aluminates at the interface BC/TBC during pre-oxidation leads to an improved adherence between TBC and TGO.

The comparison of the thermal cycling results of parameter A-D shows that continued deposition with low rate or a further reduction of the feed rate does not lead to an additional improvement of durability. The lifetimes and inverse BC temperatures follow the same trend line

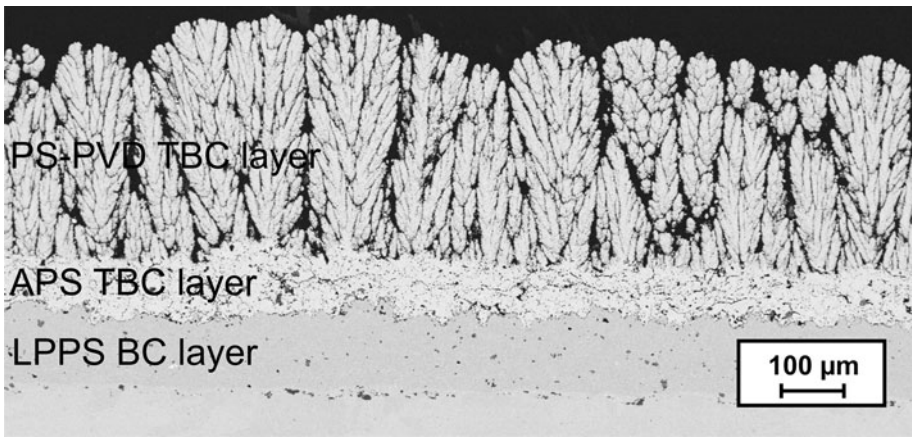

Fig. 5 Scanning electron micrograph (back-scattered electron image) of double-layer system with 50 µm APS layer

(Fig. 6). In procedure E the extended pre-oxidation was performed but no low deposition rate step was included. Two of the three specimens of this procedure show an improved durability (in a test at 1400 °C). The data points are appropriate to the same trend line as the specimens with steps of low deposition rate. The lifetime of the other specimen of procedure E, which is lower than those of APS-coatings might be an outlier.

One parameter that affects the correlation between the lifetime and the inverse BC temperature is the activation energy of the TGO growth according to Ref 8. In Fig. 7, the thickness of the TGO, which was measured from micrographs of the tested specimens after failure, is plotted against the hours of thermal cycling.

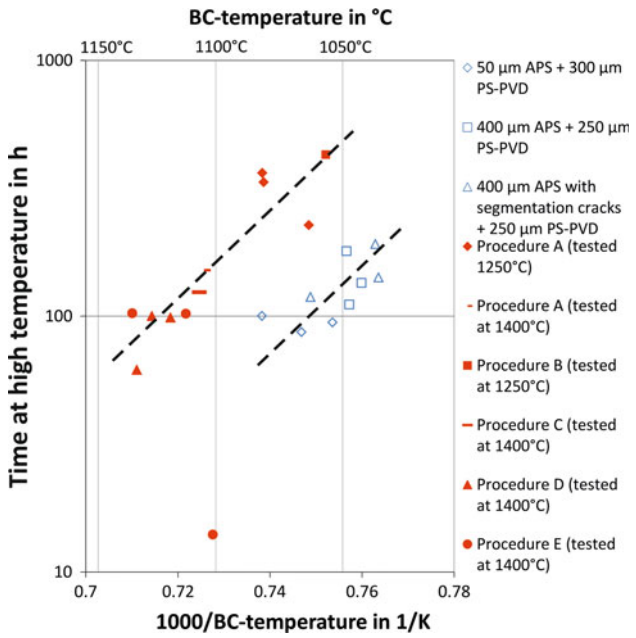

Fig. 6 Plot of lifetime in thermal cycling against the inverse bondcoat temperature

The specimens of parameter A-E show high thicknesses of the TGO layers as a consequence of the long lifetimes. Until now PS-PVD coatings did not reach such high testing times and huge TGO growths. Usually, spallation occurred earlier. The adjusted processing and the pre-oxidation seem to improve the adhesion between the TGO and the PS-PVD TBC and apparently change the growing conditions of the TGO.

When the double-layer systems are compared to one another, a higher coating thickness of the overall double-layer system leads to a lower TGO thickness, which is the reason for the lifetime differences between the three double-layer systems. Also a higher density of the coatings (segmented APS in comparison to normal APS) has a similar effect. However, the overall lifetimes of the double-layer systems are not higher compared to usual APS-coatings.

3.3 Microstructures After Thermal Cycling

Typical micrograph obtained by scanning electron microscopy of a specimen by procedure A after thermal cycling for more than 350 h at 1250 °C surface/1050 °C substrate temperature is shown in Fig. 8. A noticeable feature of the microstructure is the formation of the TGO layer. While the TGO layer seems to be homogeneous at large areas of the specimen, at some locations the growth of the TGO does not occur in a uniform way.

Occasionally, the TGO bulges out and even raises the TBC on top of it (Fig. 9). This mechanism may be controlling the lifetime of the coating. The bulging of the TGO leads to cracks in the bottom layer of the TBC and to its detachment from the BC. Next to the areas of the coating that spalled off, such bulged areas of the TGO are always found. In these zones other features of the TGO and the BC are also noticeable. The TGO is usually more rooted to the BC. Many parts of the TGO have grown inside the BC and are visible underneath the bulged zone. This phenomenon is sometimes referred to as ''pegs'' (Ref 9).

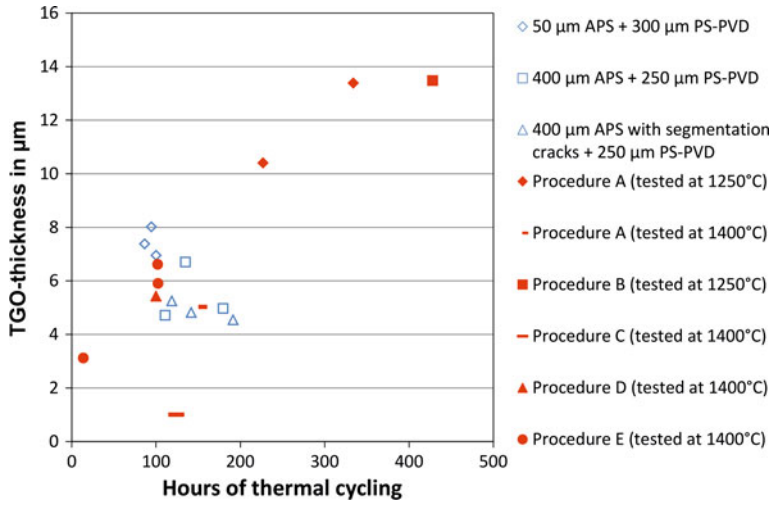

Fig. 7 Plot of TGO thickness vs. lifetime in thermal cycling

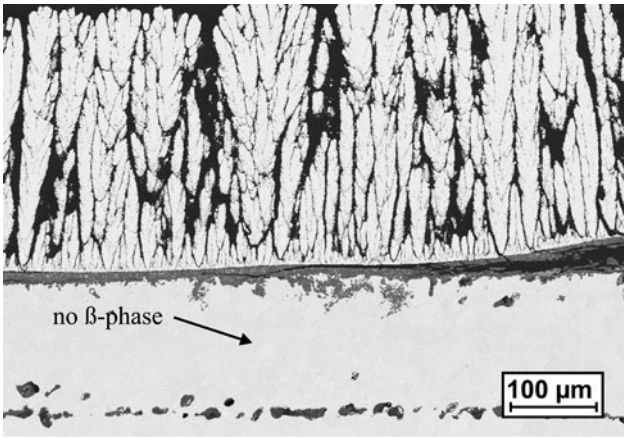

Fig. 8 Scanning electron micrograph (back-scattered electron image) of coating deposited with procedure A after failure in thermal cycling

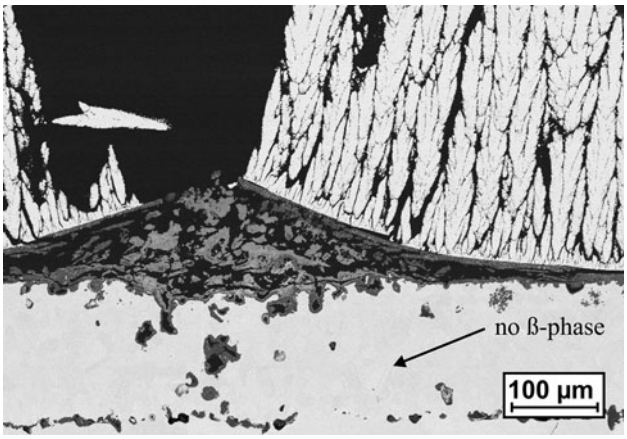

Fig. 9 Scanning electron micrograph (back-scattered electron image) of coating deposited with procedure A after failure in thermal cycling

In addition, the Al depletion zone of the β-phase in the BC is more pronounced in these areas. Sometimes there is almost absence of this phase, which serves as a reservoir of Al for the formation of the TGO layer during service/testing. It is formed as a blocky precipitation in the BC (Fig. 10). It is reported that if no aluminum is left in a BC for the formation of slow growing oxides like Al_2O_3, faster growing oxides like Cr_2O_3 and spinels (Ref 10-12) are formed. Therefore, these depleted zones might cause the growth of faster growing oxides and thereby even be the reason for the bulging of the TGO. In Fig. 8 and 9 the BC is completely depleted and no β-phase is left. At other areas on the specimen without bulging of the TGO, the BC is not completely depleted and residual zones of β-phase are observed.

In Fig. 10 a micrograph obtained by laser optical microscopy of a double-layer specimen (50 µm APS TBC layer) is shown after failure in thermal cycling at 1250 °C/1050 °C.

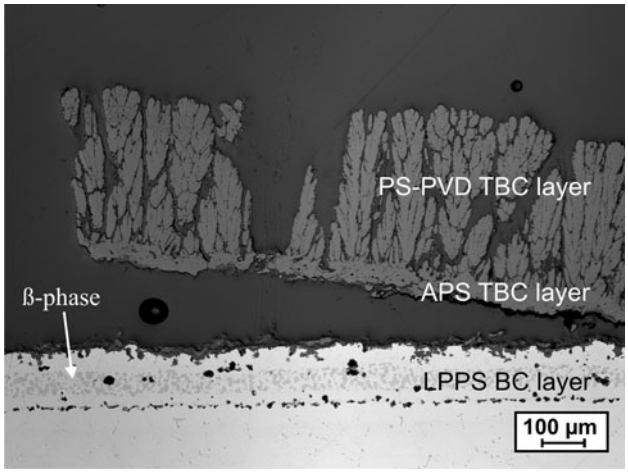

Fig. 10 Laser optical micrograph of double-layer system with 50 µm APS TBC layer after failure in thermal cycling at 1250 °C/1050 °C

The propagation of the lifetime-determining crack happened close to the interface of the TGO and the bottom APS-layer and leads to a detachment of the coating. This failure mechanism is known for TBCs made by APS. It is noticeable that the presumed good adherence between the PS-PVD and the APS-layer is confirmed. But the lifetimes of the coatings with the double-layer structures, which are in the range of usual APS-coatings, show that the double-layer structure is not an improvement compared to the conventional APS-system.

3.4 Turbine Vane Coating

Figure 11 shows the laser micrographs of the microstructures, in the as-sprayed condition, which were deposited along the stainless steel turbine vane mock-up. The deposition process was performed using the same plasma conditions that were used to coat the thermal cycling specimens. The plasma consisted of 30 slpm Ar and 60 slpm He and a current of 2600 A was set. During the deposition the mock-up was rotated with 60 rpm. It is obvious that the deposition of columnar microstructures at every location was successful. The deviation of the coating thicknesses around the profile is noticeable. Cross sections were made in four different locations along the length of the turbine vane. The first cross section (I) was made at 1.5 cm from the top of the turbine vane. Other sections (II, III, IV) are cut at 1.5 cm intervals. The lowest cross section (IV) is shown in Fig. 11.

In Table 3, the coating thicknesses which were obtained from all micrographs are summarized.

The highest coating thickness values are found at the trailing edge and at the leading edge where the convex surface curvature is highest. Similar coating thickness profiles have been reported for PS-PVD deposition on turbine vane geometry (Ref 1, 13). The flow around the rotating turbine vane and the formation of stagnation zones in the plasma plume cause this variation of thickness.

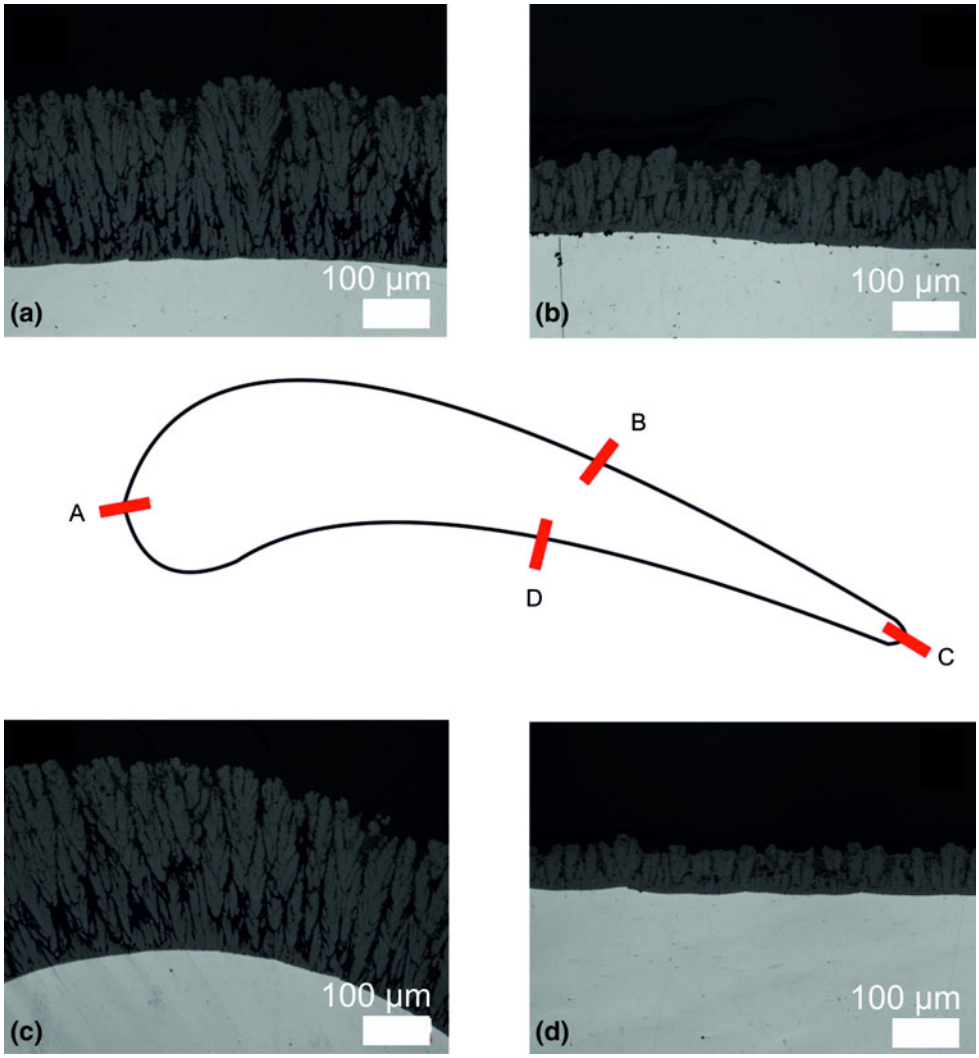

Fig. 11 Laser optical micrographs of coating on a turbine vane mock-up

Table 3 Coating thicknesses across turbine vane geometry

	Position			
Cross section	A Leading edge	B Convex side	C Trailing edge	D Concave side
I	311 µm	169 µm	313 µm	143 µm
II	281 µm	167 µm	350 µm	136 µm
III	290 µm	158 µm	292 µm	151 µm
IV	259 µm	128 µm	287 µm	78 µm

4. Conclusions

By introducing processing steps of low deposition rate and an extended pre-oxidation, the lifetime of TBCs made by PS-PVD could be increased. For such coatings, improved thermal cycling lifetimes, more than two times higher than conventionally sprayed TBCs, could be achieved in burner rig tests. By looking at the microstructures after thermal cycling, a complete depletion of the BC and a bulging of the TGO was found leading to the spallation of the coating. This failure mechanism was first observed for PS-PVD TBCs here and seems to occur only after very long periods of testing. The deposition on a turbine vane geometry showed natural variations of the coating thickness around the profile. However the coating microstructures were homogeneously columnar.

Acknowledgments

The authors gratefully acknowledge the co-operation with Dr. A. Barth, Dr. H.-M. Höhle and Dr. M. Gindrat, all Sulzer Metco.

References

1. K. von Niessen and M. Gindrat, Plasma Spray-PVD: A New Thermal Spray Process to Deposit Out of the Vapor Phase, *J. Therm. Spray Technol.*, 2011, **20**(4), p 736-743

2. M.F. Smith, A.C. Hall, J.D. Fleetwood, and P. Meyer, Very Low Pressure Plasma Spray—A Review of an Emerging Technology in the Thermal Spray Community, *Coatings*, 2011, **1**, p 117-132
3. A. Hospach, G. Mauer, R. Vaßen, and D. Stöver, Columnar-Structured Thermal Barrier Coatings (TBCs) by Thin Film Low-Pressure Plasma Spraying (LPPS-TF), *J. Therm. Spray Technol.*, 2011, **20**(1-2), p 116-120
4. A. Hospach, Untersuchungen zum Thin Film Low Pressure Plasma Spraying (LPPS-TF) Process, Ph.D. Thesis (in German), Ruhr-Universität Bochum, 2012
5. G. Mauer and R. Vaßen, Plasma Spray-PVD: Plasma Characterization and Impact on Coating Properties, *J. Phys.: Conf. Ser.*, 2012, **406**, p 012005
6. A. Refke, D. Hawley, J. Doesburg, and R.K. Schmid, LPPS Thin Film Technology for the Application of TBC Systems, *Thermal Spray 2005: Thermal Spray Connects: Explore its Surfacing Potential,* E. Lugscheider, Ed., May 2-4, 2005 (Basel, Switzerland), ASM International, 2005, p 438-443
7. F. Traeger, R. Vaßen, K.H. Rauwald, and D. Stöver, Thermal Cycling Setup for Testing Thermal Barrier Coatings, *Adv. Eng. Mater.*, 2003, **5**(6), p 429-432
8. F. Traeger, M. Ahrens, R. Vaßen, and D. Stöver, A Life Time Model for Ceramic Thermal Barrier Coatings, *Mater. Sci. Eng., A*, 2003, **358**(1-2), p 255-265
9. H.X. Zhu, N.A. Fleck, A.C.F. Cocks, and A.G. Evans, Numerical Simulation of Crack Formation from Pegs in Thermal Barrier Systems with NiCoCrAlY Bond Coats, *Mater. Sci. Eng., A*, 2005, **404**, p 26-32
10. E.P. Busso, H.E. Evans, Z.Q. Quian, and M.P. Taylor, Effects of Breakaway Oxidation on Local Stresses in Thermal Barrier Coatings, *Acta Mater.*, 2010, **58**, p 1242
11. A.G. Evans, D.R. Mumm, J.W. Hutchinson, G.H. Meier, and F.S. Petit, Mechanisms Controlling the Durability of Thermal Barrier Coatings, *Prog. Mater. Sci.*, 2011, **46**, p 505
12. D. Stöver and C. Funke, Directions of the Development of Thermal Barrier Coatings in Energy Applications, *J. Mater. Process. Technol.*, 1999, **92-93**, p 195
13. M. Goral, J. Sieniawski, S. Kotowski, M. Pytel, and M. Maslyk, Influence of Turbine Blade Geometry on Thickness of TBCs Deposited by VPA and PS-PVD Methods, *Arch. Mater. Sci. Eng.*, 2012, **54**(1), p 22-28